Supplementary Information

Surface Modification of Gold by Carbazole Dendrimers for Improved Carbon Dioxide Electroreduction

Sota Yoshida[1], Masaki Sampei[1], Naoto Todoroki[1], Eri Hisamura[2], Kohei Nakao[2], Ken Albrecht[2] and Toshimasa Wadayama[1]*

[1]Graduate School of Environmental Studies, Tohoku University, 6-2-2 Aramakiaza-Aoba Aoba-ku, Sendai 980-8579, Japan

[2]Institute for Materials Chemistry and Engineering, Kyushu University, 6-1 Kasuga-koen, Fukuoka, 816-8580, Japan

E-mail: naoto.todoroki.b1@tohoku.ac.jp

ORCID: https://orcid.org/0000-0003-4811-6398

1 · Experimental procedures

Au disk electrode

A polycrystalline Au disk electrode (ϕ = 5mm) embedded in poly-ether-ether-ketone resin (AUE, BAS) was used as a working electrode for an H-type electrochemical cell. The surface of the Au electrode was polished using alumina pastes (0.3, and 0.05 μm) and then rinsed with acetone and ultrapure water before surface modification by the carbazole dendrimers (CDs).

Au-GDL electrode

Au-GDL electrodes for a gas diffusion electrode (GDE) cell were prepared by radio frequency magnetron sputtering on a gas diffusion layer (GDL; MFK-A, Mitsubishi Chemical). The base pressure of a sputtering chamber was ~10^{-7} Pa. The one-inch-size sputtering gun (ASG-1, AVC) and Au target (99.99 %, ϕ =1 inch, t = 1mm, PLASMATERIALS) were used for the sputtering. The sputtering rate was estimated using a quartz crystal microbalance (INFICON) set in the chamber.

Carbazole dendrimers (CDs)

Carbazole (G1Cz) was purchased from Acros Organics and used after recrystallization from toluene. 9-Phenylacarbaozle (G1Ph) was purchased from TCI and used without further purification. G3Cz was synthesized according to literature.[1] G3Ph were synthesized according to literature from corresponding carbazole dendrons.[2] The NMR spectra were obtained using JEOL JNM-ECA600 (600 MHz) or Bruker AVANCE III 400 (400MHz) with TMS as the internal standard. The MALDI TOF-MS data were obtained using a JEOL JMS-S3000 in the spiral positive ion mode with Dithranol as the matrix.

Surface modification of Au electrode by CDs

The polished Au disk electrode surface was electrochemically cleaned by applying triangle wave potential cycles between 0.05-1.7 V vs. RHE. The cleaned electrode was rinsed by ultrapure water and dried in air. After that, 40 μL toluene solution (99 %, Wako) with 0.1 mM in concentration of each CD was drop-casted on the electrode and dried in air for 30 min. This process was repeated twice to prepare the modified-Au electrodes. Similar dropping and drying procedures by CDs are adopted also for Au-GDL electrode.

Electrochemical CO_2 reduction by using H-type cell configuration

A potentio-galvanostat (SP-50eZ, Biologic) equipped with an impedance module was used for the electrochemical measurements. A glass-made H-type cell, Pt-wire, and reversible hydrogen electrode were employed as the electrochemical (EC) cell, counter electrode, and reference electrode, respectively. The anode and cathode compartments (both 50 mL) were separated using a Nafion membrane (NR212; Chemours). Initial electrochemical surface cleaning of the Au disk electrode and the reduction experiments were conducted in a 0.1 M $KHCO_3$ solution at 20 °C. The 0.1 M $KHCO_3$ solution was prepared from a $KHCO_3$ powder (>99 %, ACS grade, Merck) and ultrapure water (Milli-Q).

Electrochemical measurement procedures for H-type Cell

The CO_2 electrochemical reduction was performed in CO_2-saturated 0.1 M $KHCO_3$ solution (pH = 6.8) for the Au disk electrode. The CO_2 gas (＞99.995 %) was flow into electrolyte during the electrolysis with a constant flow rate of 30 sccm (standard cubic centimeter per minute; S48-32, HORIBA STEC). The constant potential electrolysis was performed at −0.3, −0.4, −0.5, −0.6 vs. RHE for 10 min, and generated gaseous products of CO_2 reduction were analyzed by gas chromatography with thermal

conductivity detector, flame ionization detector and methanizer (GC-2014, Shimadzu). Liquidus products were analyzed by nuclear magnetic resonance (NMR) spectroscopy (JEOL, ECZL-600). Because no liquidus reduction products of CO_2 were detected for all the samples at all the applied potentials by NMR, only the faradaic efficiency of gaseous product of CO was discussed in this study.

The potential-dependent hydrogen evolution reaction (HER) behaviors were discussed by linear sweep voltammetry at a scan rate of 5 mV s^{-1} in Ar-purged 0.1 M phosphate buffer solution with pH = 6.8 (without CO_2 saturation), which the same value of CO_2-saturated 0.1 M $KHCO_3$ solution. The solution was prepared from NaH_2PO_4 ・ $2H_2O$ (>99 %, Fujifilm), Na_2HPO_4 ・ $12H_2O$ (>98 %, Fujifilm) and Milli-Q water.

Underpotential deposition of Pb

Pb-underpotential deposition experiment was performed for estimating active surface areas for each crystal facets of polycrystalline Au electrode. A polymethyl pentene (PMP) cell, Pt-wire, and Hg/HgO (0.1 M NaOH) were used as a Pb-UPD electrochemical cell, counter electrode, and reference electrode, respectively. Cyclic voltammetry was conducted between −0.75 and −0.15 V vs. Hg/HgO in Ar-purged 1 mM $Pb(OAc)_2$ + 0.1 M NaOH solution (pH = 13). The solution was prepared from

$Pb(OAc)_2 \cdot 3H_2O$ (Fujifilm, >99.9 %), NaOH (Fujifilm, >98 %) and Milli-Q water. The working electrode potential vs. Hg/HgO was converted to RHE standard using the following equation.

$$E_{RHE}\,(V) = E_{Hg/HgO} + 0.926 + 0.05916pH$$

X-ray photoelectron spectroscopy (XPS)

Chemical bonding states of the CD-modified Au electrode surface was discussed by using X-ray photoelectron spectroscopy (XPS; Theta Probe, Thermo Fisher Scientific) with a monochromatized Al X-ray source (1487 eV).

High current density CO_2 electrochemical reduction by using GDE cell

A flow-type gas diffusion electrode (GDE) cell and solution circulation system[3] was constructed in our laboratory and used for a high current density electrolysis (~100 mA cm^{-2}). Each chamber (Fig. 4(a)) in the main manuscript of cathode, anode, and CO_2-flow was made of polytetrafluoroethylene (PTFE). Pt-wire, and reversible hydrogen electrode were used as the counter and reference electrode, respectively. The cathode and anode chambers were separated using a Nafion membrane (NR212; Chemours). The 1 M $KHCO_3$ solution at 20 °C was prepared from a $KHCO_3$ powder (>99 %, ACS grade,

Merck) and ultrapure water (Milli-Q), and was used for catholyte and anolyte. The CO_2-flow rate was set to be 20 sccm by the mass flow controller (S48-32, HORIBA STEC). The applied potentials were not iR-corrected.

2・Supplemental results

CVs of Pb-UPD and HER activity for G1Cz- and G3Cz-modified Au disk electrodes

Cyclic voltammograms of the Pb-UPD experiments for G1Cz- and G3Cz-modified Au disk electrodes are presented in Figure S1(a). Estimated Pb-stripping charges from (a) are summarized in (b). The estimated charges of G1Cz-, G3Cz-modified Au disk electrodes show almost the same tendency to corresponding G1Ph, G3Ph-modified Au ones (Fig. 3 in manuscript), irrespective of the introduced functional groups (-NH and -phenyl) to the corresponding CD backbones. Figure S1(c) shows linear sweep voltammograms of G1Cz- and G3Cz-modified Au electrodes. HER current density of G1Cz-Au disk electrode slightly increased, while G3Cz-modifed Au decreased compared with non-modified one.

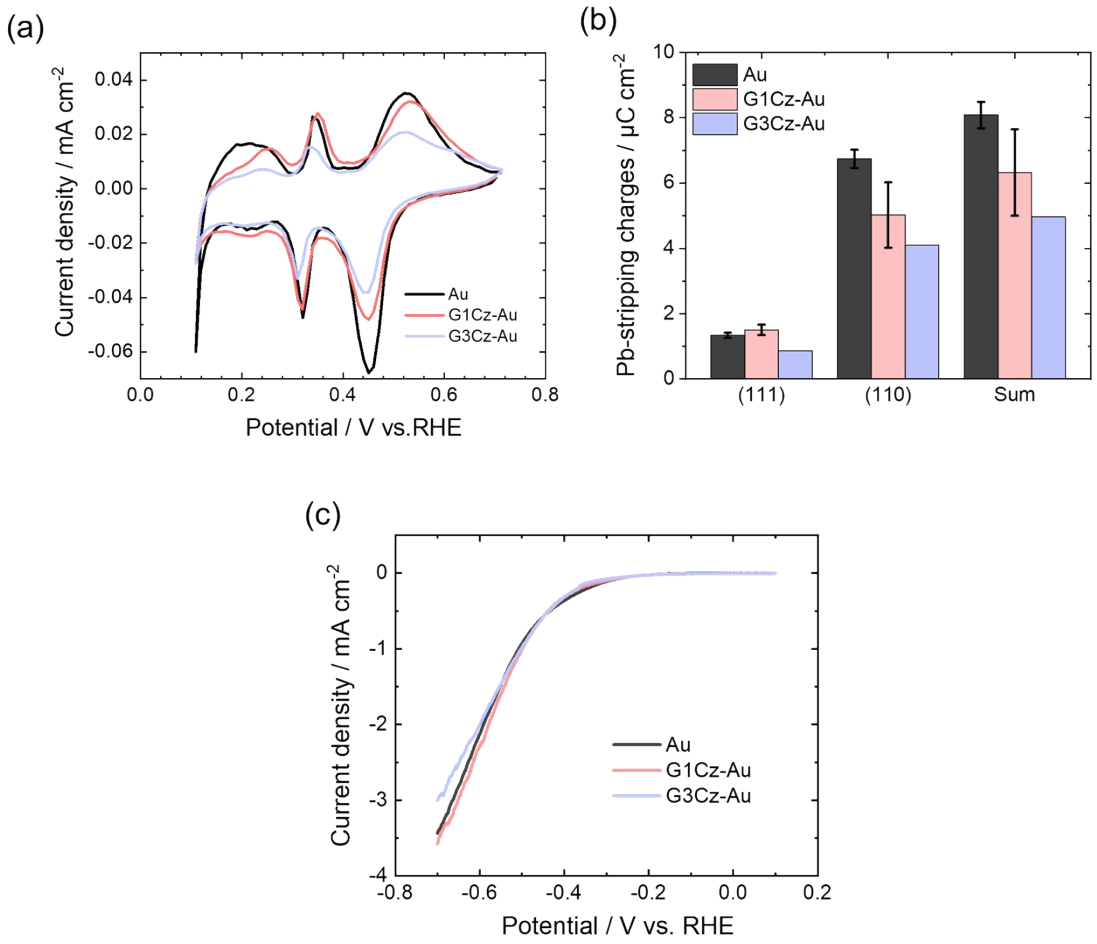

Figure S1. (a) Cyclic voltammograms collected in an Ar-purged 1 mM $Pb(OAc)_2$ + 0.1 M NaOH solution for Pb underpotential deposition. (b) Pb-stripping charges estimated from (a). (c) Linear-sweep voltammograms recorded in Ar-purged 0.1 M PBS electrolyte with a pH of 6.8 for evaluating the HER property.

NMR and MALDI-TOF-MS spectra of G3Ph and CzG3

Figure S2-S5 shows NMR and MALDI-TOF-MS spectra of G3Ph and CzG3.

No impurities could be detected for the synthesized G3Ph and CzG3 used in this study.

(a)

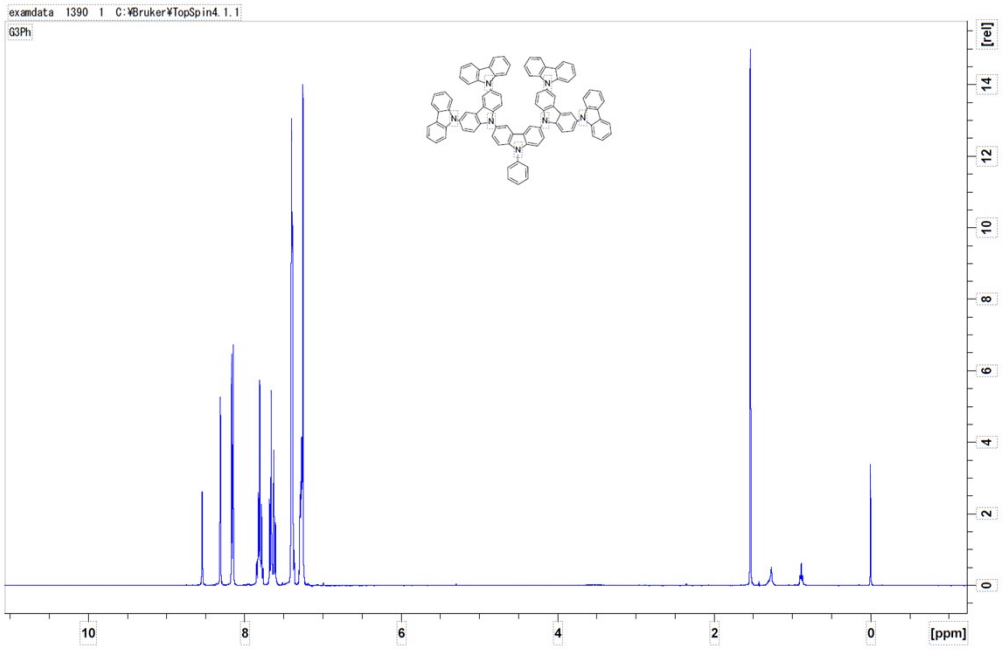

(b)

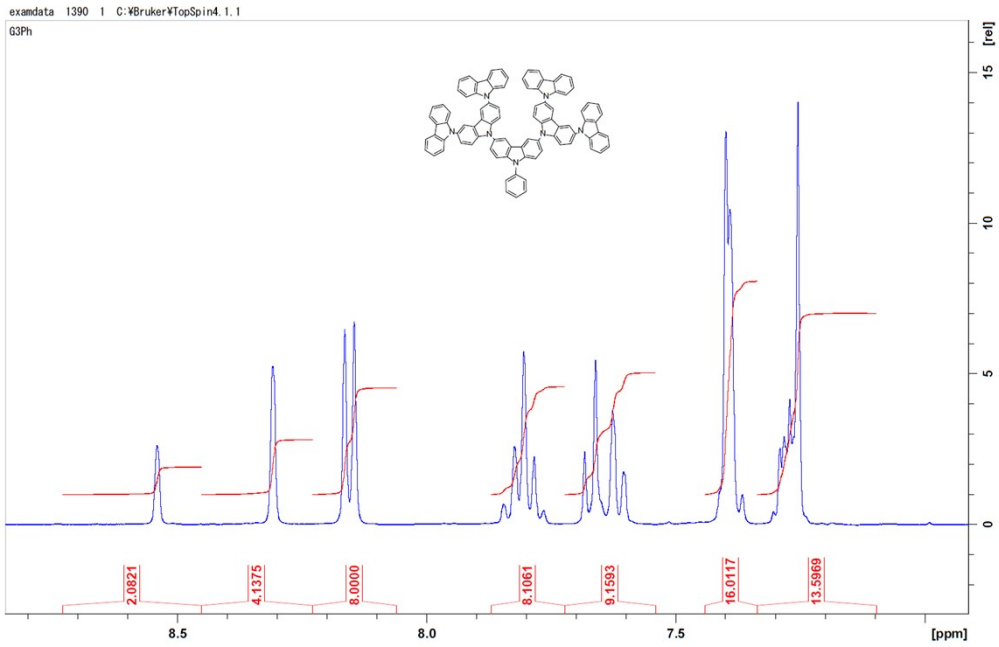

Figure S2. ^{1}H NMR spectrum of G3Ph in chloroform-d: (a) overall, (b) enlarged spectrum.

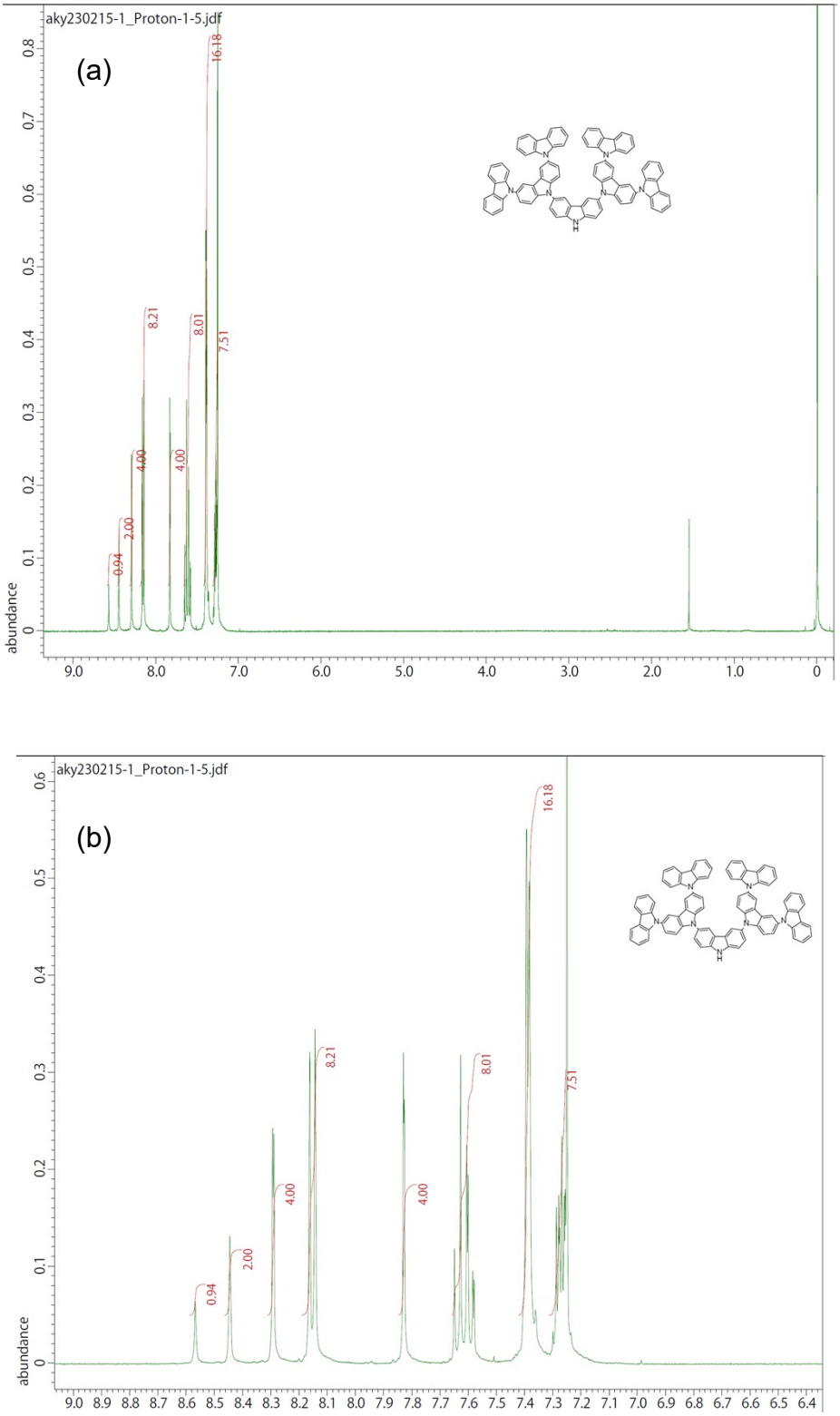

Figure S3. ^{1}H NMR spectrum of G3Cz in chloroform-d: (a) overall, (b) enlarged spectrum.

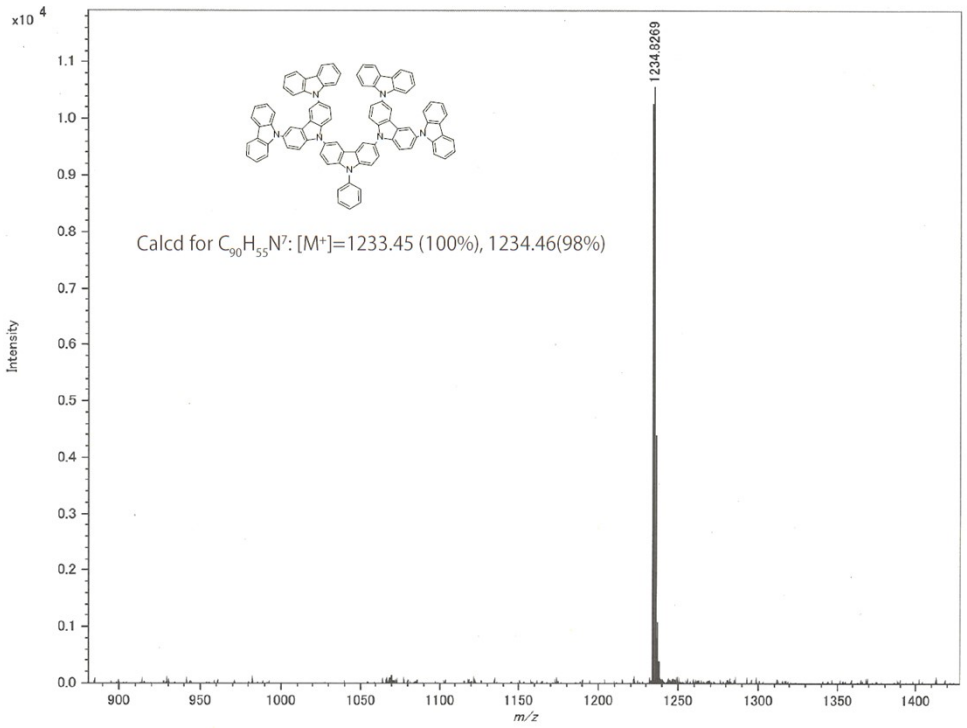

Figure S4. MALDI-TOF-MS spectra of G3Ph.

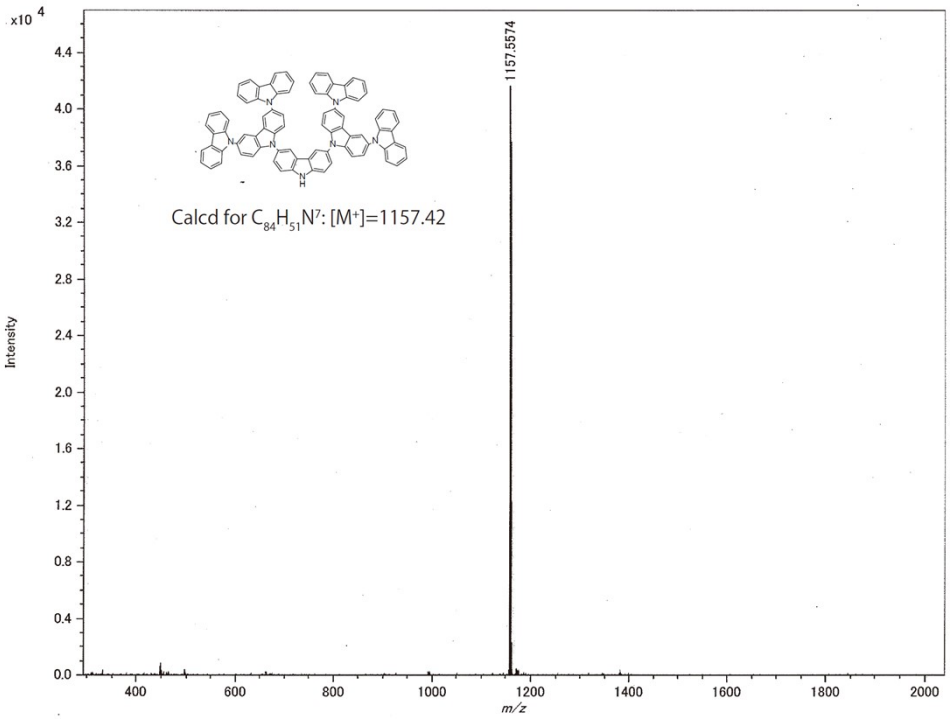

Figure S5. MALDI-TOF-MS spectra of G3Cz.

3. Comparison of the FE_{CO} and j_{CO} with previous studies

Tabel S1. Summary of FE_{CO} and j_{CO} values for molecular-modified Au surfaces reported to date.

Sample	Surface modifiers	Electrolyte	FE_{CO}		Partial current density for CO		Ref.
			Max. value	Potential vs. RHE	Max. value	Potential vs. RHE	
Au nanorod	5-mercapto-1-methyltetrazole	0.5 M $KHCO_3$	98	-0.6	14.5	-0.9	4
Au nanofibers	polyaniline	0.1 M $NaHCO_3$	70	-0.7	6.9	-0.9	5
Au-NPs/N-doped carbon	L-cysteine	0.1 M $KHCO_3$	95	-0.75	27	-0.95	6
Au-NPs/C	PTFE	0.1 M $KHCO_3$	95	-0.7	8.4	-1	7
Au-NPs/rGO	Oleylamine	0.1 M $KHCO_3$	75	-0.7	7.4	-0.8	8
Au-NPs/C	PVA	0.5 M $KHCO_3$	97	-0.58	98.6	-0.77	9
Au-NPs/C	Porphyrin ligand P1	0.1 M $KHCO_3$	93	-0.45	7.9	-0.8	10
Au disk	G1Ph	0.1 M $KHCO_3$	98	-0.4	2.8	-0.6	This study
100nm-Au/GDL		1 M $KHCO_3$	99	-0.7	98	-1.7	
Au disk	non-modified	0.1 M $KHCO_3$	93	-0.6	2.4	-0.6	
100nm-Au/GDL		1 M $KHCO_3$	89	-0.5	87	-1.7	

References

1. K. Albrecht, K. Matsuoka, K. Fujita and K. Yamamoto, *Angew. Chem. Int. Ed.*, 2015, **54**, 5677-5682.
2. K. Albrecht and K. Yamamoto, *J. Am. Chem. Soc.*, 2009, **131**, 2244-2251.
3. M. Sassenburg, R. de Rooij, N. T. Nesbitt, R. Kas, S. Chandrashekar, N. J. Firet, K. Yang, K. Liu, M. A. Blommaert, M. Kolen, D. Ripepi, W. A. Smith and T. Burdyny, *ACS Appl Energy Mater*, 2022, **5**, 5983-5994.
4. J. Wang, J. Yu, M. Sun, L. Liao, Q. Zhang, L. Zhai, X. Zhou, L. Li, G. Wang, F. Meng, D. Shen, Z. Li, H. Bao, Y. Wang, J. Zhou, Y. Chen, W. Niu, B. Huang, L. Gu, C. S. Lee and Z. Fan, *Small*, 2022, **18**, e2106766.
5. T.-H. Wang, C.-Y. Lin, Y.-C. Huang and C.-Y. Li, *Electrochim. Acta*, 2023, **437**, 141500.
6. M. Tan, X. Han, S. Ru, C. Zhang, Z. Ji, Z. Shi, G. Qiao, Y. Wang, R. Cui, Q. Luo, J. Jiao, Y. Li and T. Lu, *Nano Research*, 2022, DOI: 10.1007/s12274-022-4878-3.
7. J. H. Lee, S. Kattel, Z. Xie, B. M. Tackett, J. Wang, C.-J. Liu and J. G. Chen, *Advanced Functional Materials*, 2018, **28**, 1804762.
8. Y. Zhao, C. Wang, Y. Liu, D. R. MacFarlane and G. G. Wallace, *Adv. Energy Mater.*, 2018, **8**, 1801400.
9. L. Ma, W. Hu, Q. Pan, L. Zou, Z. Zou, K. Wen and H. Yang, *Journal of CO2 Utilization*, 2019, **34**, 108-114.
10. Z. Cao, S. B. Zacate, X. Sun, J. Liu, E. M. Hale, W. P. Carson, S. B. Tyndall, J. Xu, X. Liu, X. Liu, C. Song, J.-h. Luo, M.-J. Cheng, X. Wen and W. Liu, *Angew. Chem. Int. Ed.*, 2018, **57**, 12675-12679.